PILOT MODELLING FOR DEPARTURE AND WAKE VORTEX RECOVERY USING NEURAL NETWORKS

S. Amelsberg, D. Bieniek, R. Luckner
Technische Universität Berlin, Institute of Aeronautics and Astronautics
Marchstrasse 12, 10587 Berlin, Germany
S. Kauertz , Airbus Deutschland, Flight Dynamics
Kreetslag 10, 21129 Hamburg, Germany

ABSTRACT

This paper describes the development of a pilot model (PM) that is able to perform the take-off run, rotate, follow a standard instrument departure route and recover and stabilize the aircraft during and after a wake vortex encounter. It can be used in fast-time Monte-Carlo simulations with varying wake vortex encounter conditions for safety analyses. The PM generates sidestick pitch, sidestick roll, pedal, throttle lever, flap lever, and landing gear lever commands and manipulates those control elements as a pilot would do. For each control element a sub model is developed. The sub models for sidestick pitch and roll commands are modelled by artificial neural networks (NN). Those for pedal position, flap, landing gear, and throttle lever use classical control schemes and are only described briefly here, since the focus of the paper lies on the PM's neural network sub models. A further part of the PM is a disconnect logic that disables the auto pilot (AP) during wake vortex encounters in automatic flight if the pilot decides to counteract and recover from the vortex-induced disturbances manually. For design and validation of the NN sub models, data was generated in a certified A330 Full Flight Simulator and A320 development simulator with licensed commercial airline pilots. For final validation, the PM was implemented into the real-time flight simulator and it flew identical encounters as the airline pilots before. This allowed comparing the PM outputs with the human pilot control commands.

NOMENCLATURE

Symbols

p	Roll rate
q	Pitch rate
Φ	Bank angle
Θ	Pitch angle
ψ	Azimuth
γ	Path angle
Γ	Vortex Circulation
H	Altitude above ground
b	Span
x	Pos. coordinate with ref. to the longitudinal axis
y	Pos. coordinate with ref. to the lateral axis
z	Pos. coordinate with ref. to the yaw axis

Indices

cmd	command
disc	disconnect
gr	Geodetic system
PM	Pilot Model
targ	Target
WV	Wake Vortex

Abbreviations

AAM	Average Angle Measure
A/C	Aircraft
AP	Auto Pilot
A/THR	Auto Throttle
FAR	False Alarm Rate
FCOM	Flight Crew Operating Manual
FD	Flight Director
HTR	Hit Rate
ICAO	International Civil Aviation Organization
MCS	Monte Carlo Simulation
MSE	Mean Square Error
NN	Neural Networks
PM	Pilot Model
POP	Probability of prediction
SID	Standard Instrument Departure Route
TUB	Technische Universität Berlin (TU Berlin)
WVE	Wake Vortex Encounter

1 INTRODUCTION

The CREDOS (Crosswind- Reduced Separation for Departure Operations) project, funded by the European Commission, studies the concept of reduced wake turbulence separation between consecutive departing aircraft for single runway operations [1]. For the validation of this concept, a risk assessment is required. The chosen method computes wake vortex encounter probabilities and encounter severities by means of fast-time Monte Carlo simulations (MCS). This approach is commonly used for risk assessment as real-time pilot-in-the-loop simulations are too time consuming and therefore not suitable for MCS. The aim of the MCS is to assess the potential impact of the proposed reductions in separation on flight safety and the efficiency of airport operations in crosswind conditions. As simulation results shall be used to revise separation standards without negative impact on safety, they have to be accepted by the authorities. Therefore all models need to have a high fidelity and strict validation requirements apply for all parts of the simulation including the aircraft model, the aircraft vortex interaction model and the model for the pilot control behaviour.

As a part of CREDOS, Technische Universität Berlin (TU Berlin) is developing pilot models (PM) for risk assessment that shall mimic the pilot's control behaviour when tracking a Standard Instrument Departure (SID) route and when compensating the disturbances of a wake vortex encounter. Data for PM development was recorded in flight simulator tests, in which pilots experienced vortex

encounters during climb out. The tests were performed on an Airbus A330 Level D Full-Flight Simulator and on an A320 development simulator. Commercial pilots from several airlines with varying flight experience participated in the tests.

The objective is to develop a pilot model that performs take-off, departure and wake vortex recovery, that can be used in Monte Carlo simulations, and that is suited for the CREDOS risk assessment. Pilot model design is based on the data acquired during the piloted WVE simulations.

2 FLIGHT SIMULATOR TESTS

Two flight simulators were used to investigate piloting techniques and pilot control behaviour:

- The Airbus A330 Full-Flight Simulator that is located at TU Berlin, Institute of Aeronautics and Astronautics and is operated by the "Zentrum für Flugsimulation Berlin" (ZFB).
- The A320 THOR Simulator, an Airbus development simulator, is located at Airbus Deutschland GmbH in Hamburg.

Both simulators are equipped with research facilities that allow efficient modifications of the simulator software for scientific experiments. The simulator software has been supplemented with the wake vortex encounter software package that was developed in the S-WAKE (Assessment of Wake Vortex Safety) project [6]. This allows highly realistic simulations of wake vortex encounters. A major difference is that the A330 simulator has a motion system whereas the THOR simulator is fixed-based. The importance and limits of motion simulation during wake vortex encounters was investigated in [2] reporting indications that pilot behaviour is affected by the cues from motion simulation. However, a final conclusion was not drawn as the statistical data base was too small. Therefore the hypothesis here is that the impact of motion on pilot response lies within the statistical variations.

Using the simulation tool WakeScene [4], a number of different test cases for the piloted simulator campaigns were developed that cover the most probable encounter conditions during take-off. Test cases are defined by the encounter geometry, encounter altitudes and vortex characteristics. The test scenarios were the same for both simulators and the conditions are given in TAB 1. For each test run, a constant crosswind was defined that is typical for a CREDOS scenario. The aircraft parameters are summarized in TAB 2.

Scenery	Frankfurt/Main airport (EDDF)
Runway	25R – 249°
SID	TOBAK2F
Crew	Pilot flying from the left or right hand seat; supported by an engineer
Visibility	CAVOK
Wind QNH Ceiling	190° / 10kt 1013.5hPa 0/8

TAB 1: Simulator test scenarios

	A320 THOR simulator (Airbus)	A330 FFS (TUB)
A/C type	A320-200	A330-300
A/C gross weight	66000 kg	160000 kg
CG	25% MAC	28% MAC
Thrust rating	Flex 42	Flex 62
V_{Rot}	137 kts (Flaps 2)	126 kts (Flaps 2)
V_2	142 kts (Flaps 2)	133 kts (Flaps 2)

TAB 2: Aircraft data for simulator tests

During a simulator campaign, the pilots were flying departures, in which they experienced wake vortex encounters that varied in magnitude and character. As pilots' actions on the controls should be recorded, they were asked to fly most departures manually. However, some departures were flown automatically, i.e. with Autopilot (AP) engaged, to investigate when and why a pilot disconnects the AP during a vortex encounter.

For validation, requirements are needed that quantify the allowable differences between the reactions of the pilot model and human pilots. As human pilots have a typical scatter in their control actions, it was necessary to identify how wide the variations are. This was addressed by repeating certain representative test scenarios 5 times per pilot. The results allowed assessing the typical scatter per pilot when repeating a test and the scatter in between pilots when flying the same scenario. To guarantee identical vortex-induced disturbances, those cases were flown as "Fixed Encounters". In a Fixed Encounter, fixed (pre-recorded) vortex-induced forces and moments act on the aircraft, no matter what the actual flight path is. Thus vortex-induced disturbances are identical for each test; only variations in pilot action can cause the scatter in aircraft reaction. Vortex-induced forced and moments were recorded on a former test campaign, in which encounter geometries and encounter characteristics were defined such that they result in roll encounters of varying strength and duration, see TAB 3. In a test session the Fixed Encounter cases were repeated randomly without notifying the pilot.

Name	$\Delta\gamma_{WV}$	$\Delta\psi_{WV}$	Γ	b_{WV}	WV_{RL}	H_{WV}
FXE	[°]	[°]	[m²/s]	[m]	[ ]	[ft]
224b	0	-5	500	55	1	656
0227	-6	-10	650	55	1	900
0223	5	0	500	55	-1	1100
0231	-5	-5	750	55	0	656
224a	-5	-1	500	55	1	656
0212	-9	5	500	160	-1	165

TAB 3: Fixed encounter cases

$\Delta\gamma_{WV}$ Vertical encounter angle
$\Delta\psi_{WV}$ Lateral encounter angle
Γ Vortex circulation
b_{WV} Vortex span
WV_{RL} WV reference line definition: +1=Left vortex, -1=Right vortex, 0=Center between vortices

H_{WV} Encounter altitude above ground level

The parameters defining the encounter geometry are visualised in FIG 1.

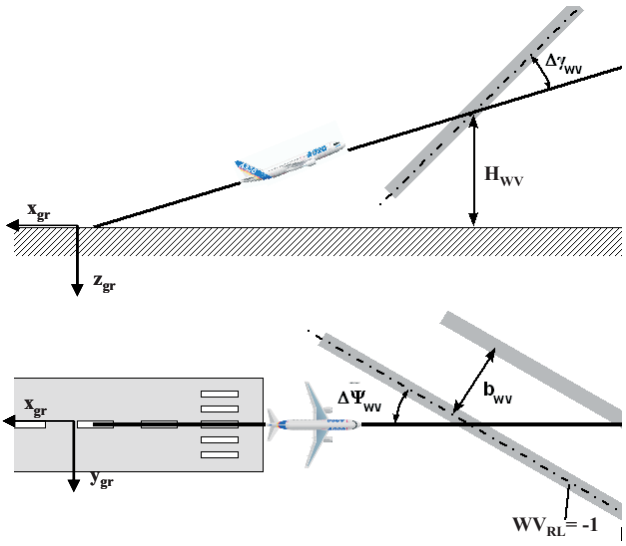

FIG 1: Wake vortex encounter geometry

In summary, 15 simulator sessions were carried out in the A330 simulator. 11 different airline pilots (6 captains, 5 first officers) flew 690 wake vortex encounters in total. On the A320 simulator, a total of 576 wake vortex encounters in 14 simulator sessions with 14 different pilots (5 captains, 9 first officers) were flown.

3 PILOT MODEL

For standard departure route tracking and wake vortex recovery, a pilot model is developed for offline flight simulation that performs the following control tasks:

- Take-off run on the runway centre line,
- Rotation,
- Climb along the desired flight path,
- Correct lateral deviations,
- Match the stationary aircraft climb gradient to the actual thrust level,
- Maintain required aircraft speed by thrust control,
- Stabilize the a/c after encountering a wake vortex.

The pilot model is structured into the following sub-models:

i. Ground tracking,
ii. Rotation,
iii. SID tracking,
iv. Wake vortex recovery,
v. Flap, landing gear, thrust lever control.

It controls the following elements:

i. Sidestick pitch,
ii. Sidestick roll,
iii. Pedal position,
iv. Throttle lever (TL),
v. Flap lever (FL),
vi. Landing gear lever (LGL),
vii. AP disconnect model.

FIG 2 gives an overview of all sub models of the pilot model. Part of it is a mode management logic that selects sub models according to flight phase piloting procedures and switches to a recovery mode if a vortex encounter occurs. The first switch is between manual and automatic flight modes. In the automatic mode the upper loop is active, where the block AP controls the aircraft (block A/C) until the AP disconnect sub model switches to the manual mode. In manual departures either the blocks Take-off run, Rotation, SID tracking or wake vortex recovery can be active at one time, whereas the Flap /LG and Thrust lever models are active in parallel during the whole departure phase. Vector $\underline{c}$ contains the sidestick pitch and roll control as well as pedal position, where $\underline{c}_{AP}$ stands for the auto pilot commands and $\underline{c}_M$ for the manual pilot model commands. Vector $\underline{d}$ includes throttle, flap, and landing gear lever.

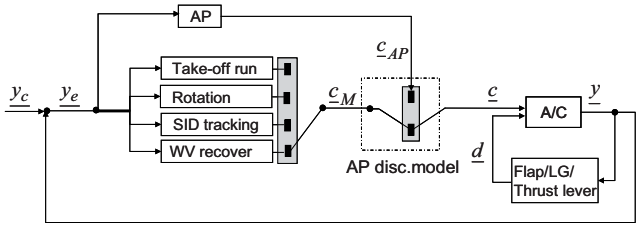

FIG 2: Sub models of pilot model

Sidestick pitch and roll commands that are outputs of the Rotation, SID tracking, and WV recovery model, are modelled with a static feed-forward neural network. The other outputs provided by the sub models for Take-off run, Flap /LG and Thrust lever are based on simple algorithms and logics as functions of speed, altitude, pilot time delay, and Flight Director command. The following sections describe all the sub models in more detail.

3.1 Ground tracking

In cross-wind conditions the pilot uses the pedals to control the aircraft on the runway centre line until rotation. The pedal command δ_{Pedal} is computed as a function of Flight Director yaw command FD_{yaw} and a pilot lag time τ_P.

(1) $$\delta_{Pedal} = f(FD_{yaw}, \tau_P)$$

3.2 Rotation

Pilots rely on visual attitude information and acceleration cues. Based on these considerations the pilot behaviour during rotation is modelled by using a low-gain pitch rate law. Pitch rate command increases from 0 deg/s to a target pitch rate depending on the aircraft's attitude; and then decreases back to 0 deg/s when reaching θ_{target} =15 deg. This concept has been augmented by a second order time delay, modelling the smooth character of pilot inputs. The rotation control mode is active from the time the aircraft reaches the rotation speed until achieving the target pitch rate. The pitch rate command q_{cmd} is computed with respect to rotation speed V_R and target pitch rate q_{targ} as follows

$$q_{\mathrm{cmd}} = S_{VR} \cdot q_{\mathrm{targ}} \cdot \frac{1}{T_R^2 \cdot s^2 + 2T_R s + 1}$$

(2) Switch $S_{VR} = 0$ for $V < V_R$

$$S_{VR} = 1 \text{ for } V \geq V_R$$

From the available validation data, a range of 0.4 s ≤ T_R ≥ 0.8 s, was identified; for subsequent analysis the mean value T_R = 0.6 s will be used. Sidestick pitch deflection δ_{col} is computed according to the law

(3) $$\delta_{\mathrm{col}} = (q_{\mathrm{cmd}} - q) \cdot K_{q1}, \text{ for } \Theta < \Theta_{\mathrm{targ}}$$

Reasonable results were obtained for gains K_{q1} within a range of 1.0 ≤ K_{q1} ≤ 3.0. Here the mean value of K_{q1} = 2 is used. At a given offset from the target pitch attitude, rotation control smoothly transitions to tracking mode. The SID tracking model is a neural network and is described in detail in section 3.4.5. The pilot model needs default values for rotation speed V_R, target pitch rate q_{targ}, and the target pitch angle θ_{targ}. The values depend on aircraft type and configuration.

3.3 Flap, landing gear and thrust lever

The thrust control function is based on the piloted simulator test and the Flight Crew Operating Manual (FCOM). In a performance calculation, the correct thrust parameters for each aircraft, the defined takeoff configuration and environmental conditions were computed. Airlines train their pilots to use flexible thrust settings for take-off to increase engine life time and reduce maintenance cycles and costs. Based on the general operational procedures, the throttle lever deflection δ_{TL} and the landing gear lever position δ_{LGL} are determined as a function of altitude H above ground and a pilot lag times τ_{TL} and τ_{LGL} which assume different values. The flap lever deflections δ_{FL} depend on altitude H and calibrated airspeed V, as well as on a pilot lag time τ_{FL}.

(4) $$\delta_{TL} = f(H, \tau_{TL})$$

(5) $$\delta_{LGL} = f(H, \tau_{LGL})$$

(6) $$\delta_{FL} = f(H, V, \tau_{FL})$$

3.4 Neural Network modelling

Reference [8] explains Neural Networks (NN) as follows: Artificial NNs are mathematical models that emulate biological nervous systems and are composed of a large number of interconnected processing elements, similar to neurons. The elements are connected via weights that are analogous to synapses, which serve as the junction through which neurons communicate with each other. The synaptic connections are adjusted by learning processes in biological systems. A priori input and output data is needed for the development and training of the NN. In training process the data sets are used to adjust net's parameters.

A major advantage of a Neural Network (NN) is that it can be trained to behave like a given non-linear dynamic system. Thus, NN can be used to model complex systems, like non-linear human behaviour.

In this paper an artificial NN is applied to the mathematical modelling of human pilot sidestick control inputs. The experimental data for NN design and training was gathered in the piloted simulator tests as described in section 2. The following subsections describe the theoretical background for NN design and the development of the NN for sidestick roll and pitch command in detail.

3.4.1 Neural net topology

The structure of an artificial static feed-forward neural network with one hidden layer is shown in FIG 3. The first layer of a NN is termed the input layer (index *i)*. The activation function f can be found in the hidden layer (index *j)*. The activation function which is generating the final output signal is denoted the output layer marked with index *k*.

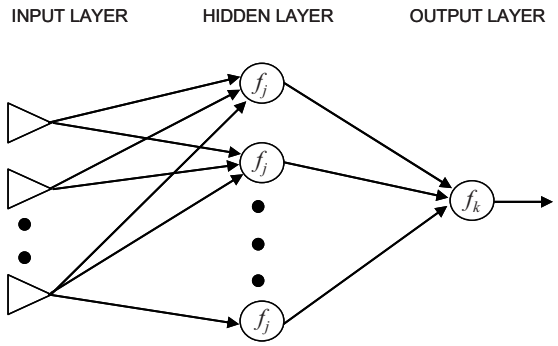

FIG 3: Neural network topology

A network is created by the combination of a few simple artificial neurons where an artificial neuron can be mathematically described as a processing element, as it is given in FIG 4.

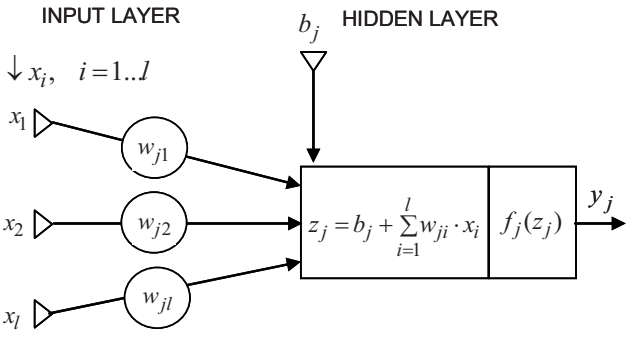

FIG 4: Structure and function of a processing element

Where x_i is the input, w_{ji} is the weight between input and hidden layer, b_j is the bias in the hidden layer, $f_j(z_j)$ is the activation function in the hidden layer, and y_j is the output of the hidden layer.

Mathematically, the operation of a network of processing elements can be presented as follows:

(7) $$z_j = b_j + \sum_{i=1}^{I}(x_i \cdot w_{ji}), \qquad y_j = f_j(z_j)$$

The output layer usually uses an identity function as activation function ($f_k=1$), therefore the output of the network y_k is generated as follows:

(8) $$y_k = z_k = b_k + \sum_{j=1}^{m}(y_j \cdot w_{kj}),$$

where b_k is the bias in the output layer and w_{kj} is the weight between hidden and output layer,

3.4.2 Neural network parameter optimization

The NN is usually trained by backpropagation in MATLAB [10]. This is a supervised learning method, which requires a number of representative input data with corresponding output data.

The network training results in an adaptation of the weight and bias matrices to minimize the cost function between the given target output data y^* and the calculated network output y_k. At time t the network weights are adapted as follows:

(9) $$w(t) = w(t-1) + \Delta w(t)$$

By training, the cost function J, that is the mean square error (MSE) between network output data and training data, is minimized.

(10) $$J = \frac{1}{N}\sum_{n=1}^{N}(y^*(n) - y_k(n))^2,$$

where N is the number of data samples.

The input weight adaptation can be described as

(11) $$\Delta w_{ji} = -\eta \frac{\partial J}{\partial w_{ji}},$$

where η is the learning rate. The layer weights change Δw_{kj} and the biases change Δb_j in the hidden layer and the bias changes Δb_k in the output layer are determined in the same way.

Eq. (11), Eq. (10), Eq. (8), and Eq. (7) show what the algorithm's name implies, the errors of the output data is propagated backwards from the output nodes to the inner nodes.

The Levenberg-Marquardt algorithm is chosen to minimize the network error. It combines the steepest descent and the Gauss-Newton method [9, p. 290-p. 294].

One of the major challenges in NN design is to guarantee the validity and generalisation of the network. Generalization means that the NN produces reasonable outputs for input signals for which it was not trained. A careful choice of network structures is necessary to avoid redundant hidden nodes that can reduce the generalisation capabilities of a network. To avoid over-fitting and to achieve a better generalization, cross validation is used in the training process. In this technique the available data is divided into three subsets. The first subset is the training set, which is used for computing the gradient and updating the network weights and biases. The second subset is the cross validation set and the third data set is used for offline verification (testing), as described in section 4.1.

In training with cross validation the mean square error of the actual NN output is calculated for the training data set as well as for the cross validation data set. The MSE of the validation set is monitored during the training process. Normally, its MSE decreases during the initial phase of training, as does the training set error. However, when the network begins to over-fit the data, the error of the validation set typically begins to rise. When the validation error increases for a specified number of iterations the training is stopped (in this case for 5 epochs in a row), and the weights and biases for the minimal validation error are returned as the optimal solution.

In addition, a post optimisation in MOPS (Multi Objective Parameter Synthesis) [4] was conducted using the average angle measure (AAM) as a second optimisation criterion; see EQ. (12) and FIG 5. As it was not possible to use self defined cost functions in MATLAB [10] for the neural net learning process, the AAM was maximized in post processing.

(12) $$AAM = 1 - \frac{4}{\pi}\left[\frac{\sum_{n=1}^{N} D(n)\cdot|\alpha(n)|}{\sum_{n=1}^{N} D(n)}\right];$$
$$\alpha(n) = \arccos\left[\frac{|y^*(n) + y_k(n)|}{\sqrt{2}D(n)}\right]; \quad D(n) = \sqrt{y^*(n)^2 + y_k(n)^2}$$

In Eq. (12) N is the number of recorded samples. D is the resulting vector length of the pilot y^* and pilot model y_k output and α is the resulting vector angle. In case of a perfect match between pilot and pilot model output, α would be 0 deg for each time step which leads to an AAM of 1.

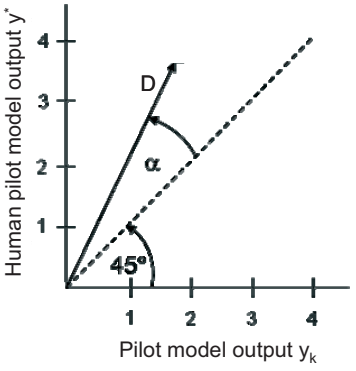

FIG 5: Definition of average angle measure

The correlation coefficient is also given here, because it is used in the next section as a parameter to evaluate how the neural network perform on the test data, but is wasn't an optimisation criterion.

(13)
$$R = \frac{\sum_{n=1}^{N}\left(y^*(n)-\bar{y}^*\right)\cdot\left(y_k(n)-\bar{y}_k\right)}{\sqrt{\sum_{n=1}^{N}\left(y^*(n)-\bar{y}^*\right)^2\cdot\sum_{n=1}^{N}\left(y_k(n)-\bar{y}_k\right)^2}}$$

y^* recorded human pilot outputs
y_k neural network modelled outputs
$\bar{y}^*, \bar{y}_k$ respective mean values of recorded and modelled pilot outputs
N number of data samples

Compared to the correlation coefficient R, which assesses only the phase characteristics between two signals, the AAM assesses magnitude and phase characteristics between the human pilot's and the modelled sidestick command. A value of 1 corresponds to a perfect magnitude and phase match, -1 implies perfect magnitude correlation but 180° out of phase, and 0 indicates that neither magnitude nor phase correlation exists.

The average angle measure is the cost function that is minimized using the genetic algorithm (GA). The weight and bias values for the minimum MSE from the backpropagation process are taken as initial values for GA optimisation. GA is a global optimization algorithm, based on evolutional strategies that guarantee the survival of the fittest individual. The selection schemes used are tournament or rank selection with a shuffling technique for choosing random pairs for mating [4]. Limited computing power leads to a formulation that input and layer weight matrices of the neural network can be adapted by the optimization algorithm and not each individual weight and bias. This is realised by a factor δ which is handled as a tuning parameter in front of the input weight matrix $\underline{\underline{w}}_{ji} = \delta_{w_{ji}} \cdot \underline{\underline{w}}_{ji}$ and the layer weight matrix $\underline{\underline{w}}_{kj} = \delta_{w_{kj}} \cdot \underline{\underline{w}}_{kj}$.
The bias in the output layer should be adapted as well in order to avoid an undesired offset. Finally, a pattern search (local gradient-free method) is used to make sure that the minimum is found, because GA is only able to converge in the region of the global minimum.

3.4.3 Pilot model inputs

The Flight Director (FD) indicates size and direction of control inputs that are required to guide the airplane along the programmed route. The Flight Director bars are displayed on the Attitude Indicator.

Especially in wake vortex operation, the pilot reaction depends on visual cues as well as on motion cues. Piloted simulator data were analysed, using correlation coefficients between selected input parameters and pilot sidestick reaction. The neural network was tested with diverse combinations of selected pilot visual and motion cues, to find the best fit for the human pilot outputs.

The following inputs were investigated for lateral control: Flight Director roll command, bank angle, roll rate, roll acceleration, and calibrated airspeed. The best results were achieved with parameter combinations of Flight Director roll command, roll rate and roll acceleration (bank angle is implicitly covered by flight director). For longitudinal control: Flight Director pitch command, pitch rate, pitch acceleration, pitch angle, sink rate, and change in sink rate were investigated. The combinations of flight director pitch command and pitch acceleration provide the highest correlation to the sidestick pitch signal.

3.4.4 Neural network for lateral control

Different net topologies were tested to achieve an optimal trade-off between a good generalisation and fitting properties for the NN pilot model. In close combination with the choice of input parameters, the following net topologies were compared: NN with one hidden layer versus a NN with two hidden layers, and between two neurons and twenty neurons in the first layer and fourteen neurons in the second layer. The second hidden layer gives no significant improvement in sidestick roll and pitch model output. The correlation between increasing the number of neurons and PM quality is non-linear. There exist some worst case combinations for the number of neurons and inputs. In general above a certain number of neurons a further increase of neurons does not significantly decrease the MSE.

Lateral control is structured into two tasks. The first is, to track the standard instrument departure route as precise as the average pilot in manual flight operations does; the second is to recover roll attitude when a wake vortex encounter occurs. Vortex recovery is a high gain task, whereas SID tracking is a low gain task, for each of which a neural network was designed.

1) For wake vortex recovery a high gain PM is needed. The NN structure was investigated as described in the paragraph above. The best trade-off between good generalization capabilities and a good fit of pilot sidestick roll inputs yield a feed-forward network for lateral control with one hidden layer and 6 neurons with *tangens hyperbolicus* activation functions as shown in FIG 5. The thickness of the lines is proportional to the magnitude of the connection weight, and the shade of the line indicates the sign of the interaction between neurons: black connections are positive and gray connections are negativ.

The NN for the lateral wake vortex recovery applied on test data achieved a correlation coefficient R= 0.9 [Eq. (13)], and the Average Angle Measure AAM= 0.67. The test data is measured simulator data which the NN never saw before, neither in training nor for cross validation.

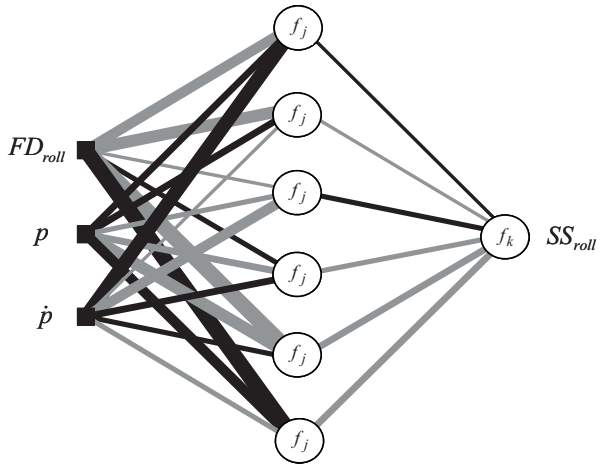

FIG 6: Neural network for lateral wake vortex recovery

2) For the tracking task where accelerations are small a simpler network, see FIG 7, with only two neurons with

Flight Director roll command and roll rate as inputs was sufficient. For the test data, it achieved a correlation coefficient R=0.7, and an AAM=0.42.

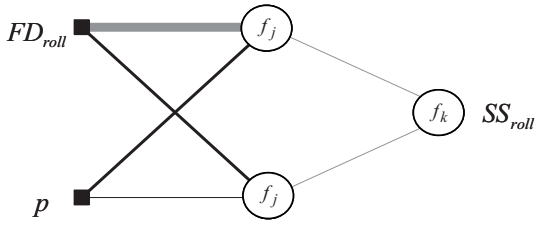

FIG 7: Neural network for lateral control (tracking)

3.4.5 Neural network for longitudinal control

Pilot model tracking tasks and wake vortex recovery in longitudinal control is addressed similarly. For both tasks, a simple feed-forward NN with one hidden layer and 4 neurons with *tangens hyperbolicus* activation functions, as given in FIG 8, delivered the best results. Applied on test data the described network achieved a correlation coefficient of R= 0.78, and an AAM= 0.47.

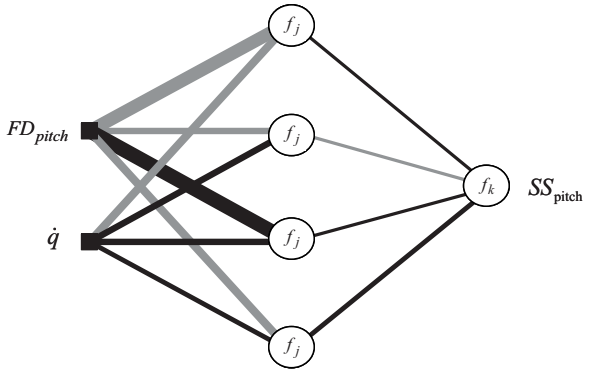

FIG 8: Neural Network for longitudinal control

3.5 Auto pilot disconnect model

The pilot model (PM) shall perform departures manually as well as automatically. In automatic flight the pilot monitors the flight situation. If excessive atmospheric disturbances cause deviations from the nominal flight path or from nominal attitudes, the pilot disables the auto pilot (AP) and recovers the aircraft manually. As wake vortex encounters can cause such deviations, a decision model for AP disconnect was developed. All automatic departures, where the pilot disconnected the auto pilot manually during the wake vortex encounter, were used to design the "AP disconnect" model. A model for Auto Throttle (A/THR) disconnect was not developed, because the auto throttle was never disconnected in all test cases.

Correlations between aircraft parameters and AP disconnect conditions have been investigated. Finally the following decision logic delivered the best results:

$$AP\_disc = f((|\Phi| > 30° \wedge |p| > 25°/s) \vee (|\Phi| > 40°) \vee (|p| > 30°/s)) \quad (14)$$

The boundaries are shown in FIG 9, together with the used test data generated from simulator tests where pilots performed automatic departures. The black dots outside the boundary mark the departures where the auto pilot was manually disconnected.

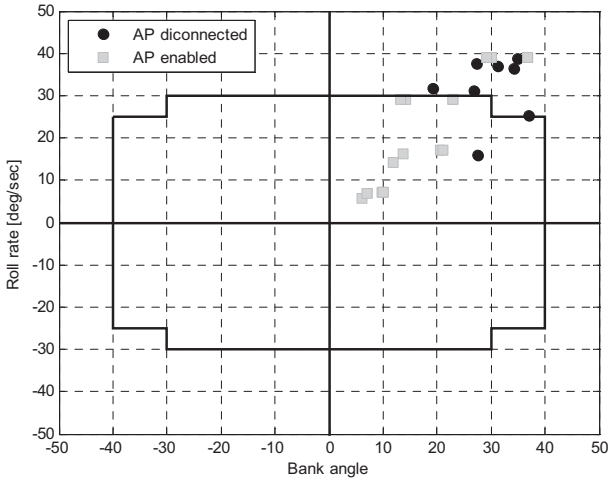

FIG 9: AP disconnect requirements

TAB 4 gives an overview on predicted capabilities. Correctly predicted were: a=15 cases for AP engaged and d=18 for AP disconnected. The prediction "AP stays enabled" was wrong in b=1 case, and "AP was disconnected" was falsely predicted in c=2 cases.

	AP enabled occurred	**AP disconnected occurred**
AP enabled predicted	a =15	b =1
AP disconnected predicted	c =2	d =18

TAB 4: AP disconnect statistic data

Criteria performance can be defined by the following indicators that are defined in [3]. The Hit Rate (HTR) represents the percentage of correct prediction.

$$\mathrm{HTR} = \frac{a+d}{a+b+c+d} \cdot 100\% \quad (15)$$

The probability of prediction (POP) is the ratio ("AP enabled" or "AP disconnected") between correct predictions to overall cases. The best value for POP is one, and the worst is zero.

$$\mathrm{POP}_{\mathrm{enabled}} = \frac{a}{a+c} \cdot 100\% \quad (16)$$

$$\mathrm{POP}_{\mathrm{disconnected}} = \frac{d}{b+d} \cdot 100\%$$

The False Alarm Rate (FAR) is the percentage of falsely predicted AP disconnects. The best FAR value is zero and the worst is one.

(17) $$\mathrm{FAR} = \frac{c}{(c+d)} \cdot 100\%$$

The achieved values are:

- HTR =92%,
- $\mathrm{POP}_{\mathrm{enabled}}$=88.2%
- $\mathrm{POP}_{\mathrm{disconnected}}$= 94.7% and
- FAR=10.0%

These values were considered to be sufficiently accurate.

4 MODEL VERIFICATION AND VALIDATION

The verification and validation of the pilot model is accomplished as described below.

4.1 Pilot model offline verification

PM verification was performed open loop, meaning there was no interaction between PM and A/C dynamics. The PM receives the pre-recorded inputs from piloted simulator test but its output does not affect the aircraft response. Verification is achieved by comparing the time histories of the PM outputs with the recorded pilot responses from the simulator tests. FIG 10 shows an example of a verification case with pilot model output superimposed over data obtained from manned simulator trials during a standard departure with a wake vortex encounter. In the beginning of the takeoff run, the aircraft stays on the runway while the pilot pushes the sidestick during aircraft acceleration (0 s < t < 18 s). The pilot model shows the same behaviour on the ground. After reaching the rotation speed, the pilot model starts to rotate (20 s -30 s) and switches over to the neural net tracking task model, which is coupled to the flight director and the roll rate (30 s -50 s). If the roll rate exceeds 5°/s the PM switches into the Wake Vortex Encounter (WVE) mode, to allow high dynamic reactions based on FD roll command, roll rate and roll acceleration for lateral control and FD pitch command and pitch acceleration for longitudinal control. Between 50 s and 60 s the aircraft is encountering a severe wake vortex (Circulation Γ=500m/s^2), the PM reacts, recovers the aircraft and stabilises the steady state condition in the longitudinal and lateral axes. At the end of the run the PM returns into the tracking task mode after the roll rate has reduced for at least 3 s below 5°/s. FIG 8 shows that the PM reacts across all subtasks during take-off and departure comparable to the real pilot.

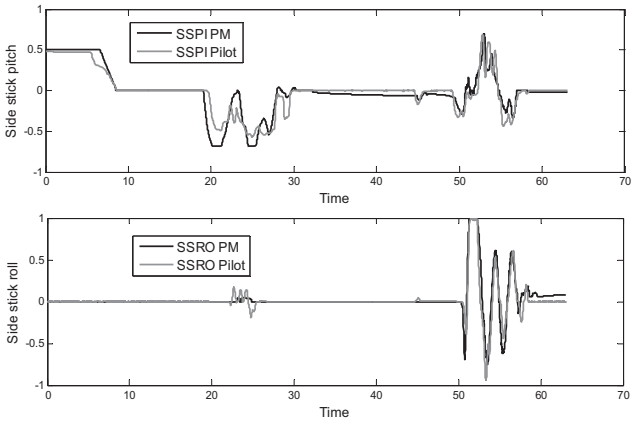

FIG 10: Pilot model (black) versus commercial pilot (grey) during take-off and departure (verification case)

4.2 Statistical analysis of variation in human pilot behaviour

For a deterministic pilot model validation, a statistical scatter of human pilot reactions is needed to demonstrate that the PM output lies within the analysed boundaries of the generated experimental data.

This section describes the identification of natural statistical scatter in pilot behaviour and the resulting aircraft motion during simulated vortex encounter. Experimental data from the “Fixed Encounter” simulator sessions, described in section 2, was evaluated. Possible requirements for the validation of pilot models are suggested. Generally, pilot response dynamics depend on the specific control task. However, other factors such as pilot training, flight experience, mental constitution, stress, and the workload, also affect pilot behaviour.

4.2.1 Scatter of time histories

For all fixed encounter cases of the piloted simulator tests, the statistical scatter was plotted as FIG 11 shows for the lateral motion parameters of case FXE 224a. These runs were performed by five different pilots who experienced identical disturbances. In general, aircraft response in the lateral axis shows similar characteristics (despite one case with oscillations caused by an over control situation). However, the variations in pilot command signals are significantly larger.

By inspecting the experimental results the following parameters are chosen for statistical evaluations: the highest amplitudes of the first noticeable sidestick roll input, bank angle, roll rate, and roll acceleration within the timeframe of encounter. For these parameters the mean values and normalized standard deviations s_{norm} are calculated for each scenario:

(18) $$s_{norm}(x) = \left(\frac{1}{n-1} \sum_{i=1}^{n} \left(\frac{x_i}{\bar{x}} - 1 \right)^2 \right)^{1/2}$$

where $\bar{x}$ is the mean value and x_i is the extreme value. The identified extreme values for each flight parameter are marked inside the vertical boundaries in FIG 11.

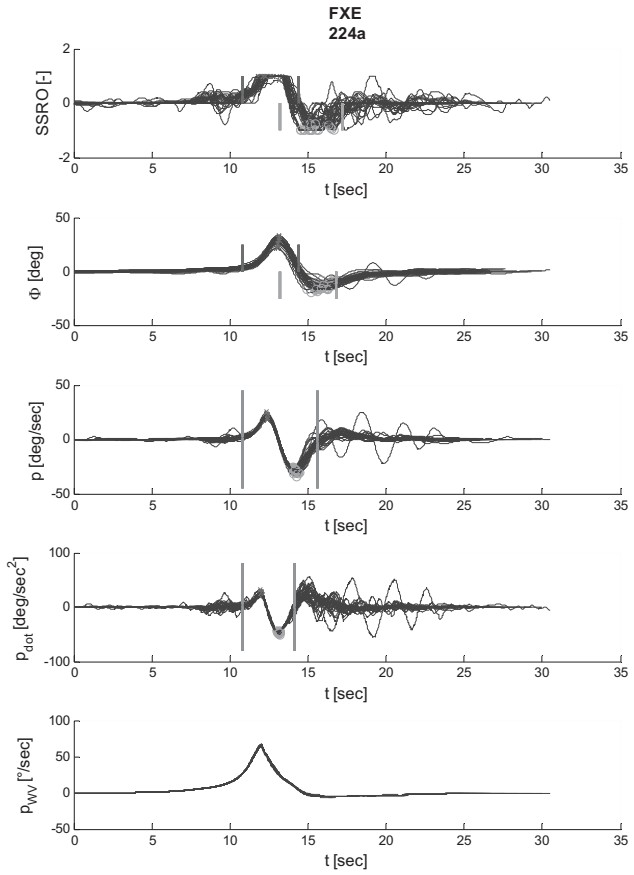

FIG 11: Statistical scatter of different pilots flying the same fixed encounter scenario (case FXE 224a)

4.2.2 Scatter of extreme values

The statistical variations of the extreme values of sidestick roll commands (FIG 12), bank angle (FIG 13) and roll rate excursions (FIG 14) are comprised in box plots that visualise the distribution characteristics for all fixed encounter cases. A box stretches from the lower hinge (defined as the 25th proportion of value distribution) to the upper hinge (the 75th proportion of value distribution) and therefore contains the middle half of the scores in the distribution. The median is shown as a line across the box. Therefore 1/4 of the distribution is between this line and the top of the box (right) and 1/4 of the distribution is between this line and the bottom of the box (left). The “H-spread” includes 95% of the analysed data and the crosses outside these boundaries mark the outliers.

The largest spread can be seen in the sidestick roll command, as expected. Distribution of bank angle and roll rate are tighter.

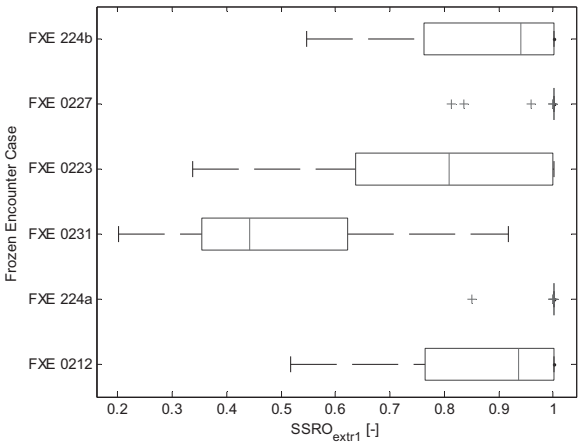

FIG 12: Box plots of the first extreme value for sidestick roll commands of six fixed encounters

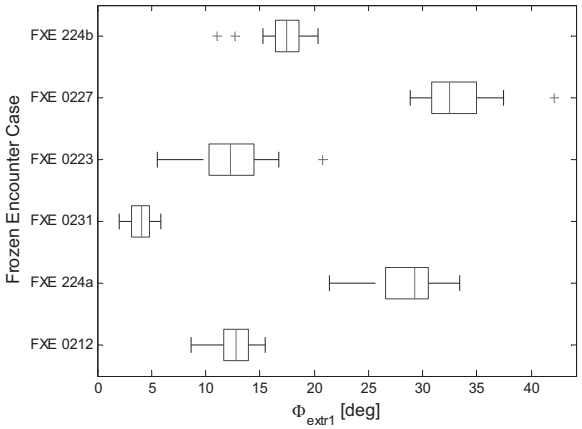

FIG 13: Box plots of extreme value for bank angle of six fixed encounter cases

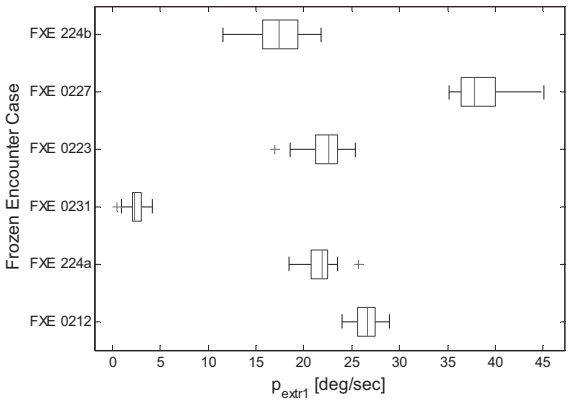

FIG 14: Box plots of extreme value for roll rate of six fixed encounter cases

TAB 5 includes the calculated mean values and the normalized standard deviations for the lateral parameters for the first and the second peak of the time histories.

FXE 224a		
	$\bar{x}$	$s_{norm}(x)$ [%]
$SSRO_{extr1}$[-]	1.0	2.76
$SSRO_{extr2}$[-]	-0.9	25.03
Φ_{extr1}[°]	28.7	10.28
Φ_{extr2}[°]	-14.8	18.81
p_{extr1}[°]	21.6	6.8
p_{extr2}[°]	-28.9	6.75

TAB 5: Mean value and normalized standard deviation

4.2.3 Requirements of pilot model validation

The pilot model is deterministic, that means for a given input parameter time history output commands are always the same. In this way it is different from a human pilot who shows variations in his response even when he is faced with identical test conditions.

The validation requirements shall guarantee that the PM is within the spread of a human pilot who is exposed repeatedly to the same encounter scenario and within the spread of different pilots during identical encounter scenarios. Especially signal characteristics that are essential for the risk assessments, for which the PM shall be used, have to be in defined bounds. For the envisaged WVE simulations the following requirements were defined:

a) The amplitudes of the first noticeable maximum and minimum sidestick roll input, bank angle and roll rate during the encounter shall not exceed the standard deviations that are determined from the validation data set.

b) The time between the maximum and minimum amplitude, shall not exceed a region of normalized standard deviation around the mean values of the validation data set.

With these requirements the maximum and minimum sidestick inputs for the given example in TAB 4 have to lie within a range of approximately 3% around the mean value in the first peak and 25% around the mean value in the second peak of the validation data.

4.3 Pilot model validation

Simulations for validation were performed with the PM in the loop, which means that the PM was implemented into the flight simulator, as opposed to the PM offline verification, where the model was tested with pre-recorded experimental data. The PM was integrated into the A320 simulator, to perform stand-alone take-off and departure simulations. The following figures give an overview of how the pilot model behaves in the flight simulation environment in comparison to the human pilots.

The sidestick roll input of pilots and PM agrees reasonably well as FIG 15 shows. The PM (black line) generates aircraft reaction as the human pilots (grey time histories). The resulting bank angle and roll rate is given in FIG 16 and FIG 17. The grey dot marks the start of the wake vortex encounter. The scatter of the first and second extreme value is also indicated and shows that the PM responds inside the pre-defined boundaries (see TAB 5).

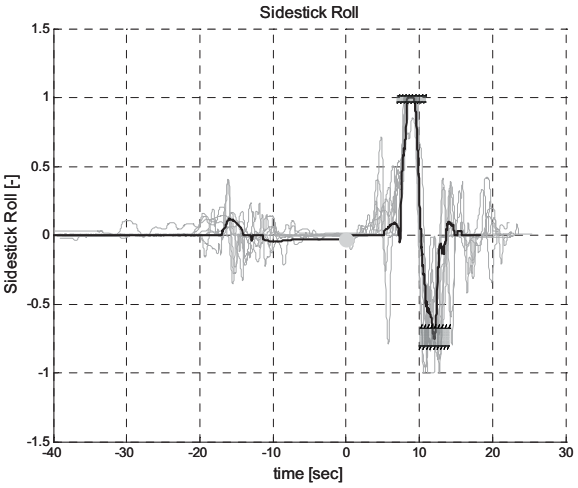

FIG 15: Pilots (grey) and PM (black) sidestick roll inputs

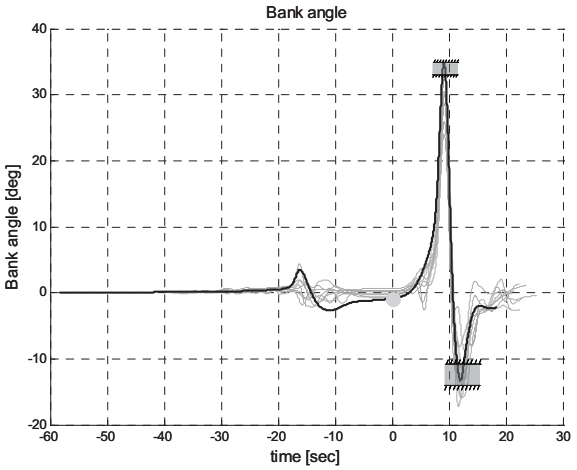

FIG 16: Bank angle resulting from inputs of pilots (grey) and PM (black)

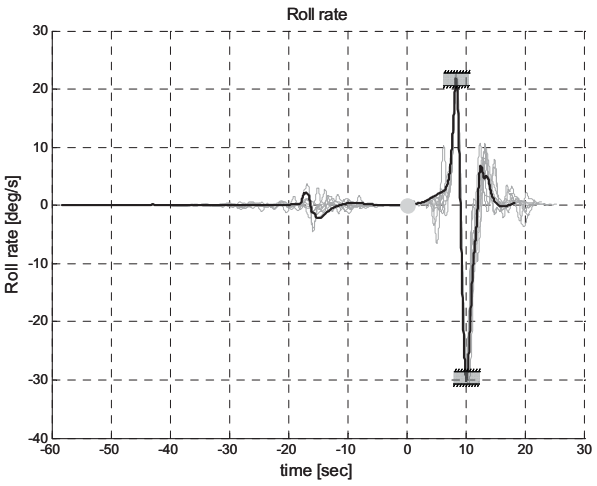

FIG 17: Roll rate resulting from inputs of pilots (grey) and PM (black)

For the longitudinal axis, recorded data show that the typical statistical scatter of human pilots is wider than in the lateral axis. A method to achieve meaningful boundaries to validate the pilot model is still in progress and no concluding results can be presented so far. However, FIG 18 shows that the PM is in good agreement

with pilot responses also for the pitch axis. The test is similar to the one that was explained in section 4.1. The PM sidestick pitch command (black line) corresponds well to a number of human pilot inputs (grey lines). The same holds for the pitch angle (FIG 17).

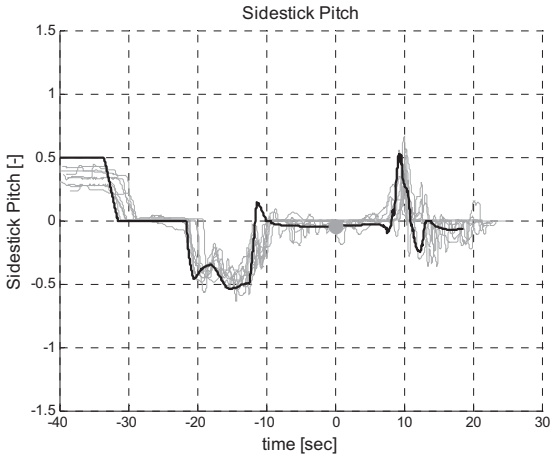

FIG 18: Pilots (grey) and PM (black) sidestick pitch inputs

The resulting aircraft reaction from PM sidestick pitch inputs is given in FIG 19.

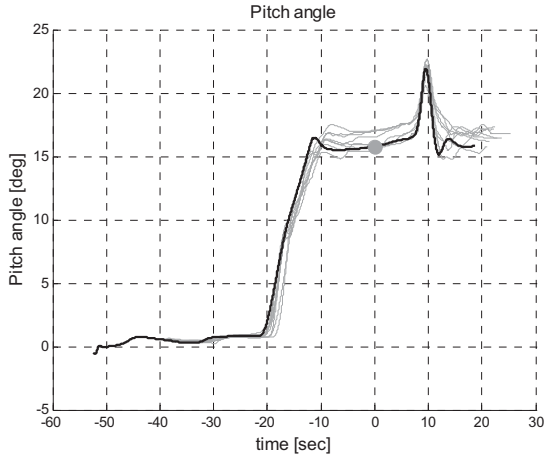

FIG 19: Pitch angle resulting from inputs of pilots (grey) and PM (black) inputs

5 CONCLUSION

The method to use fixed encounter scenarios, which generate identical vortex-induced disturbances in different test runs, turned out to be well-suited for evaluating the typical statistical scatter of human pilot behaviour.

A very good agreement between PM and human pilot behaviour is achieved in the roll axis for the A320 tests, as FIG 15 to FIG 17 show. The PM for sidestick roll commands fulfils the validation requirement during wake vortex encounters. The sidestick deflections stay inside the standard deviations at the first noticeable maximum and minimum amplitude. The same holds for the aircraft reaction in bank angle and roll rate. In the other fixed encounter cases that are not presented in this paper, the PM shows similar good results.

The definition of validation requirements for the longitudinal axis is much more difficult and not completed to date. However, a qualitative good agreement between human pilots and pilot model is obtained, as FIG 18 and FIG 19 show.

The same assessments are in progress for the A330 tests.

The described NN pilot model is deterministic that means, a given input time history always generates identical output commands. The PM provides an average behaviour of different human pilots. A next step could be the development of a probabilistic PM that addresses the individual variations of a pilot and the variations between different pilots under constant test conditions. For risk assessment analysis the PM variability could be important as it may determine worst case scenarios.

6 ACKNOWLEDGEMENTS

The work reported herein was performed within the CREDOS (Crosswind-Reduced Separations for Departure Operations) project, which was funded by the European Commission. Airbus Deutschland provided data for pilot model development and supported its validation on the A320 THOR simulator.

7 REFERENCES

[1] EUROCONTROL; *CREDOS – Crosswind- Reduced Separations for Departure Operations*; URL: http://www.eurocontrol.int/eec/credos , 06/15/09

[2] L. Fucke, R. Luckner; *Optimizing Motion Cueing for Research Flight Simulation*; CEAS-2007-330, 2007

[3] D.J. Hoad, A.O. Pickersgill*; Initial Investigations of Forecast of Wake Vortex Behaviour Classes*; Met Office, Forecasting Research Technical Report No.372, Bracknell, UK, Oct 2001

[4] D. Joos; *MOPS –Multi-Objective Parameter Synthesis V5.3*; DLR Oberpfaffenhofen, 2009

[5] F. Holzäpfel; Airspace simulation to investigate wake vortex encounter situation during take-off and departure, CREDOS D3-2, DLR Oberpfaffenhofen, 2008

[6] R. Luckner, G. Höhne, M. Fuhrmann*; Hazard criteria for wake vortex encounter during approch*; Aerospace Science and Technoloy 8 (2004) 673-687, 2004

[7] S. Amelsberg, S. Kauertz; *Piloted wake vortex encounter simulator tests for take-off and departure*, CREDOS D3-4, Airbus Deutschland, TU Berlin, 2008

[8] J. Holland*; Adaptation and Natural and Artificial Systems*, Univ. of Michigan Press, Ann Arbor, MI, 1975

[9] C.-M. Bishop; *Neural Networks for Pattern Recognition*, Oxford University Press, Oxford, 2000

[10] The Mathworks Inc.; *MATLAB (MATrix LABratory);* Version 7.5.0.342 (R2007b), August 15, 2007